Dense Branching Morphology in Electrodeposition Experiments: Characterization and Mean-Field Modeling

J. Elezgaray, C. Léger, and F. Argoul

Centre de Recherche Paul Pascal, Avenue Schweitzer, 33600 Pessac, France

(Received 5 October 1999)

Dense branching morphologies (DBM) obtained in thin gap electrodeposition cells are characterized by a dense array of branches behind a flat advancing envelope. In this Letter, we show the existence in DBM of a new (porous) phase, qualitatively different from a (compact) metal deposit. The local porosity inside the branches is found to be much more robust than geometric characteristics such as the width or the distance between branches. This fact seems to be unreported in previous modeling of DBM. A mean-field model is proposed that displays overall features observed in the experiments, such as concentration profiles, front velocity, and branched internal structure.

Electrochemical deposition (ECD) in thin cells provides, with a rather simple and elegant experimental setup, for the observation of a wide variety of morphologies, ranging from dense branching morphologies (DBM) [1] to diffusion-limited aggregation (DLA)-like patterns. Whereas DBM is characterized by a dense array of branches defining a flat front advancing at constant velocity, the DLA patterns display much more convolved geometry, with a few branches screening the growth of the others. Both can be included in the family of diffusion-limited patterns [1], characterized by the fact that the driving field satisfies the diffusion equation (Laplace's equation in the quasistationary limit) [2,3]. For instance, viscous fingering [4], dielectric breakdown, and quasi-2D combustion [5] fit into this description. In the following, we focus on experimental conditions under which the asymptotic regime is of DBM type and we develop an original approach (based on a mean-field model) in order to shed light on the morphological characteristics of these patterns.

Several models have been proposed to interpret the spatiotemporal dynamics observed in thin cell electrodeposition. Despite the fact that DBM is not homogeneous at small scales (Fig. 1), some aspects of the growth can be well described by rather simple 1D models. For instance, in Ref. [6], only the electric properties (transport of ions by migration) of the cell are considered. The approaches developed in [2,7] assume the local electroneutrality and also include diffusion terms. In particular, they predict the exponential falloff of the electrolyte concentration close to the advancing deposit, in good agreement with the experimental measurement of this profile [2]. Both approaches correctly predict the velocity of the advancing front as a function of the bulk electric field. However, these 1D models remain very global and their extension to the more realistic 2D situation is not obvious, and to the best of our knowledge has not been carried out.

In a more general context, the mere existence of DBM is somewhat puzzling, mainly because in the simplest growth models, the Mullins-Sekerka analysis [8,9] predicts the instability of the long wavelengths (the shortest ones are stabilized by some mechanism such as surface tension). Several attempts have been made to extend the simplest diffusion-limited growth model to account for the existence of DBM. In particular, the addition of dissipation (resistance, in the electric analogy) in the branches [10–12] fails to account for the stability of the planar front, and a short diffusion length in the displaced region is necessary to account for stable DBM growth [12]. However, the model studied in [12] yields a $t^{-1/2}$ time dependence of the front velocity, which has not been observed in galvanostatic ECD. From an experimental view point Zik *et al.* [5] analyzed the DBM obtained in electrodeposition experiments in light of experimental observations of fingering instabilities in quasi-2D combustion. Following this analogy they propose that the finger width (w) is current independent and that the mean distance between them is equal to the diffusion length l_D; we have shown that this hypothesis does not match our experimental measurements [13].

Another line of reasoning has been developed to understand the transition between DBM and dendritic patterns, as observed in simulations of stochastic models of diffusion-limited growth [14–16]. In particular, a mean-field model [17] has been proposed to describe the averaged properties of the overall probability distribution. It includes previous modifications of the initial mean-field model of Witten and Sander [18] as well as a generalization of the sticking rule. Remarkably, DBM is observed in this model when the 1D solution, uniformly extended to 2D, is stable. Dendrites appear when there is no uniformly moving 1D solution. It will be shown below that this mechanism for DBM fails to explain the morphologies observed in thin cell electrodeposition. More generally, all the previously mentioned models assume the existence of two clearly defined phases. This is indeed the case for solidification or quasi-2D combustion, but in electrodeposition the existence of a porous phase is a
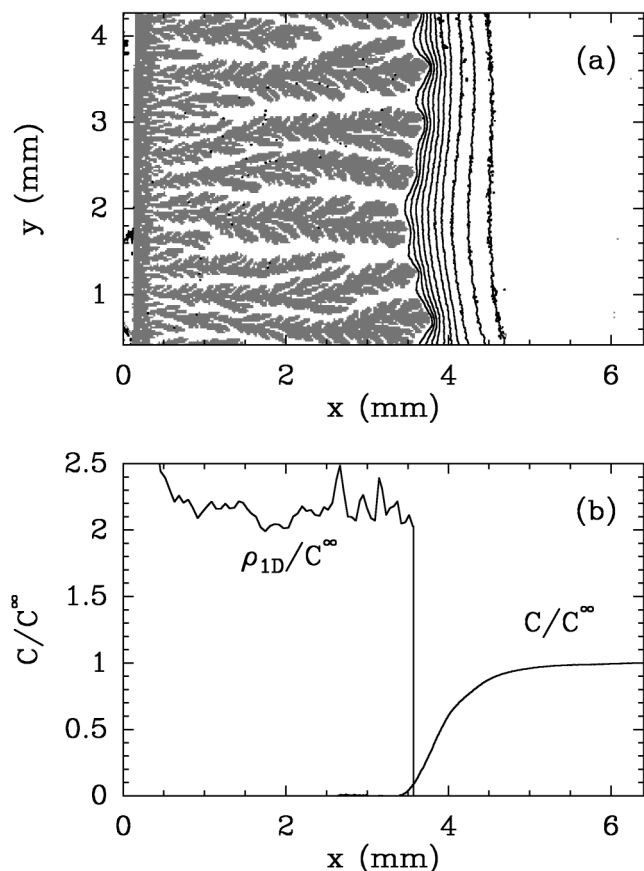
FIG. 1. (a) DBM cluster with its surrounding concentration field (contour lines with $\Delta C = C^\infty/10$), $C^\infty = [Cu(NO_3)_2] = 0.5$ mol l^{-1}, $j = -50$ mA cm^{-2}. (b) Normalized metal concentration in the deposit ρ_{1D}/C^∞ and normalized cation concentration C/C^∞ in the electrolyte, plotted versus the space variable x. ρ_{1D} has been measured from the velocity v and the diffusion length l_D by the relation: $\rho_{1D}/C^\infty = D/[(1 - t^+)v l_D]$ [13].

qualitatively new fact that can be traced to a difference in the boundary conditions at the growing interface: in solidificationlike systems, the value of the diffusive field has a well-defined value at the interface, whereas in electrodeposition, only the gradient is known. However, the *averaged* metal concentration density of the deposit ρ_{1D} of a steadily moving interface is related to the bulk concentration C^∞ through the relation [2,6,7] $\rho_{1D} = C^\infty/(1 - t_+) \simeq 2C^\infty$, where t_+ is the transference number of the cation. Therefore, ρ_{1D} is, for usual experimental conditions, much lower than the concentration of the compact metal. This new ingredient makes DBM in electrodeposition fundamentally different from previously reported DBM patterns and explains the inapplicability of previous theories. We now turn to a description of the experimental results and the mean-field model.

The experimental setup has been described in detail elsewhere [2]. All of the experiments are performed at fixed current density. The cells are made of two closely spaced optically flat glass plates ($\lambda/4$ over 50×50 mm^2) confining two straight parallel ultrapure metal wires (50 μm) which are used as both spacers and electrodes. The spacing

between the plates is fixed to 50 μm to get rid of natural convection [3,19,20]. The concentration field is measured *in situ* at each time, using a phase shift Mach-Zehnder interferometer [2] together with the geometry of the deposit. After the current is switched on, the cathodic interfacial concentration begins to decrease, and very strong potential gradients appear at the interface. Very close to Sand's time (when the interfacial concentration goes to zero), the interface becomes highly unstable [21] and develops into a forest of fine spikes that organize into well-defined fingers, as observed in Fig. 1(a). The interior of these fingers is the result of a cascade of instabilities at the μm scale, whereas the fingers themselves have a characteristic scale of the order of 100 μm. In other words, the advancing fingers are made of a "material" much more porous than that of the compact deposit [Fig. 1(b)]. The distance λ between branches is a macroscopic characteristic of the ECD clusters; we propose in [13] a method for its estimation. λ is not invariant during the growth since it can change by as much as a factor of 2 [13]. The same variability can be observed from experiment to experiment (Fig. 2). This situation is reminiscent of that found in directional solidification of alloys [22], where the same primary spacing between dendrites can be achieved with an imposed growth rate that varies by 1 order of magnitude.

Another unrelated measurable quantity is the width w of the branches, or, in an equivalent way, the fraction $\theta = w/\lambda$ of the space occupied by the (porous) metallic deposit. From our experimental study we conclude that θ has always a well-defined, current independent value that linearly depends on the bulk concentration, contrary to λ. This implies that the fluctuations in λ are necessarily correlated with fluctuations in w, in such a way that θ is conserved and that the local concentration inside a finger $\rho = \rho_{1D}\theta^{-1} = C^\infty/(1 - t_+)\theta^{-1}$ [13] is also conserved. Therefore, the μm scale porosity inside the branches seems much more robust than the value of λ. We now introduce a model that displays most of the experimentally observed features.

This model involves three different fields: the concentration of the electrolyte $C(x, y, t)$, the local density of the deposit $\rho(x, y, t)$, and the local electric potential $\Phi(x, y, t)$.
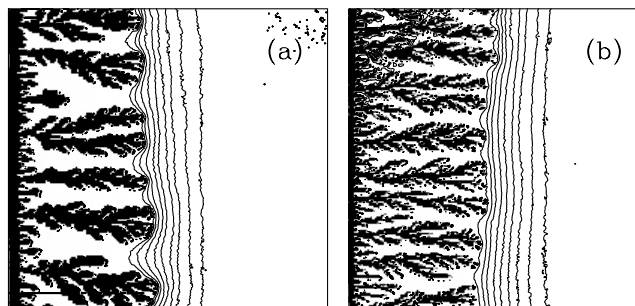
FIG. 2. Two DBM patterns with their respective concentration fields obtained with the same experimental conditions. $[Cu(NO_3)_2] = 0.5$ mol l^{-1}, $j = -25$ mA cm^{-2}, and $l_D \simeq 380$ μm, width of the pictures 5 mm.

The basic equations for C and ρ are essentially the same as those of the "aggregate field" and "diffusive field" of Ref. [17] except for the growth law which depends on the local value of Φ. More precisely, the evolution equations for C and ρ are

$$\partial_t C = \Delta C - PC \exp[-\beta(\Phi - \Phi_{\mathrm{el}})], \qquad (1)$$

$$\partial_t \rho = aPC \exp[-\beta(\Phi - \Phi_{\mathrm{el}})]. \qquad (2)$$

Here, $P = \rho^\gamma + \epsilon^2 \Delta\rho$ is a function that, roughly speaking, is concentrated around the growing zone a, β and γ are parameters of the model, and ϕ_{el} is defined below [Eq. (4)]. This form of P is directly inspired from Ref. [17] (γ models a growth cutoff at low density of walkers). There are at least two ways to (intuitively) justify Eqs. (1) and (2). First, if one replaces P by a δ function located at a sharp interface, the simplest electrodeposition model is recovered, namely, $\partial_t C = \Delta C$ in the bulk, and $\vec{n} \cdot \vec{\nabla} C = C \exp[-\beta(\Phi - \Phi_{\mathrm{el}})]$ at the interface, moving with a normal velocity given by $v_n = aC \exp[-\beta(\Phi - \Phi_{\mathrm{el}})]$. Second, one could consider Eqs. (1) and (2) as arising from some coarse-graining procedure applied to a discrete stochastic model of electrodeposition, similar to that developed in Ref. [17]. This second point of view gives some justification to the form of P. We stress the fact that the value of C at the interface is not known *a priori,* only the value $\partial_n C$ is imposed when replacing P by a delta function.

The distinctive feature of the present model is the presence of the potential field in the growth term. The equation satisfied by Φ can be straightforwardly derived from the local electroneutrality condition [23] (we assume that the diffusion coefficient of the cations and the anions is the same): $\vec{\nabla} \cdot (C\vec{\nabla}\Phi) = PC \exp[-\beta(\Phi - \Phi_{\mathrm{el}})]$. Again, replacing P by a δ function gives the boundary condition $C\vec{n} \cdot \vec{\nabla}\Phi = C \exp[-\beta(\Phi - \Phi_{\mathrm{el}})]$ of the model with a sharp interface. We have actually modified the equation for Φ by imposing that the electric field is small as soon as $\rho \neq 0$:

$$\vec{\nabla} \cdot [(C + \rho/\eta)\vec{\nabla}\Phi] = PC \exp[-\beta(\Phi - \Phi_{\mathrm{el}})],$$
$$\eta \ll 1, \quad (3)$$

which amounts to say that the branches have a nonzero (but small) resistivity. Equation (2) implies that the velocity of the growth front depends on two fields that are nonlinearly coupled through Eq. (3). Notice however that, if $P \to \delta$, the usual relation $v_n \sim \vec{n} \cdot \vec{\nabla} C$ still holds. The parameter Φ_{el} is chosen, at each time t, such that the total current

$$\int_{\mathrm{cell}} PC \exp[-\beta(\Phi - \Phi_{\mathrm{el}})] = I \qquad (4)$$

is constant in time. This corresponds to the galvanostatic conditions used in the experiments described above.

Figure 3(b) displays the typical behavior of the 1D solution of Eqs. (1)–(3) with boundary conditions: $C^\infty = 1$, $\partial_x C_{(x=0)} = \partial_x \rho_{(x=0)} = \partial_x \rho_\infty = 0$, $\Phi_{(x=0)} = 0$,

and $\partial_x \Phi_\infty = I$. Initially, the electrolyte species diffuse into the electrode (this could be prevented by making the diffusion coefficient ρ dependent) while afterwards it is progressively consumed at the "interface" (the narrow region where ρ and C coexist). Then, the system goes to a traveling wave solution, with the velocity being determined by the galvanostatic condition (4). This solution satisfies $v \partial_x \rho = aCP \exp[-\beta(\Phi - \Phi_{\mathrm{el}})]$. Integrating this relation throughout the cell leads to $v\rho_{-\infty} = aI$. The same reasoning applied to Eq. (1) leads to $vC^\infty = v = I$, thus $\rho_{-\infty} = a$ and $v = I$. The concentration profile $C(\xi, t) \simeq 1 - \exp(-\xi/l_D)$, with $\xi = x - vt$ and $l_D = I^{-1}$ fits that experimentally measured in Ref. [2]. We have performed a linear stability analysis of this steady solution by numerical means and found that the most unstable wavelength is of the order of magnitude of the diffusion length I^{-1}. In order to pursue the comparison with the experiments, we present here
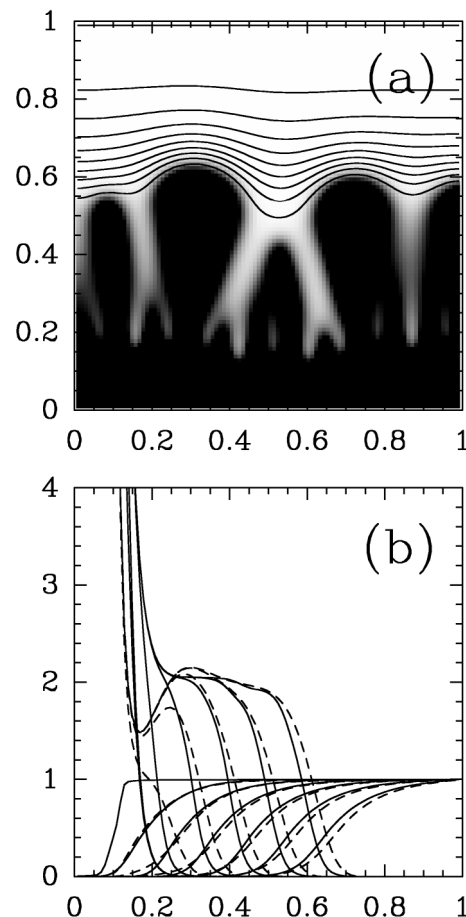
FIG. 3. Representation of a typical solution of the mean-field equations (1)–(4), with parameters $\gamma = 2$, $I = 10$, $\epsilon^2 = h^2$ (h = mesh size), and $a = 2$. (a) 2D contour map of the concentration profile (concentration difference between contour lines is 0.1) and the deposit ρ field coded in a grey scale ranging from 0 (white) to 2 (black). (b) Average (in the y direction) concentration of the deposit and the concentration fields. The dashed lines represent the solution of the 1D version of the same equations with initial conditions given (approximately) by the average initial condition of (a).
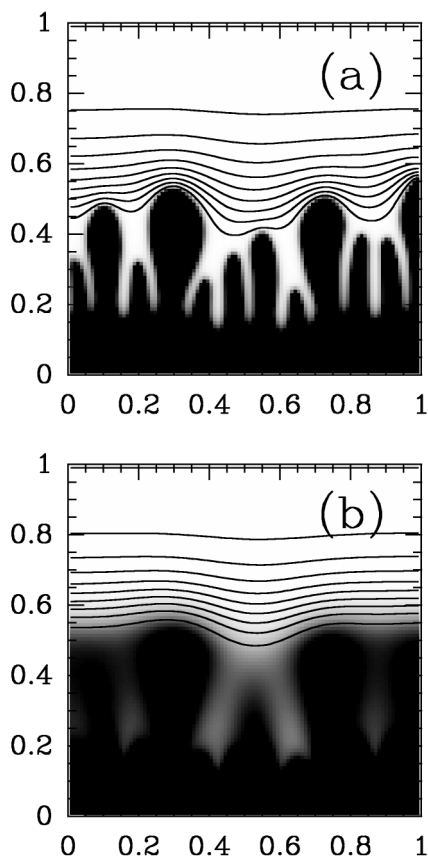
FIG. 4.   Representation of a typical solution of the mean-field equations (1)–(4), with parameters $\gamma = 2$, $I = 10$, and $a = 2$; surface tension parameter (a) $\epsilon^2 = 0.2h^2$; (b) $\epsilon^2 = 5h^2$, where h is the mesh discretization. Same coding as in Fig. 3.

numerical simulations of the full 2D equations (cf. Figs. 3 and 4). They show that initial perturbations of the 1D solution develop into well-defined "fingers," through a complex process of screening, within a global envelope that remains flat. Notice however that, contrary to what is suggested by Fig. 3(a), the branches cannot merge in a single advancing front, as the latter can be shown to be unstable. The width of these fingers is independent of the initial condition and is of the order of magnitude of the diffusion length, as in the experiments. The average concentration ρ_{1D} of the deposited zone is a [Fig. 3(b)], as expected. The parameter γ does not seem to influence much the width or the distance between branches, but rather the width of the interface. On the other hand, the width of the fingers depends critically on the value of ϵ, as shown in Fig. 4. In fact, it can be shown that the role of this parameter is analogous to a surface tension in the sense that, the bigger ϵ is, the thicker the fingers become. The experimental results mentioned above stress the fact that two control parameters are of importance, namely, the bulk concentration and the current. Correspondingly, in the rescaled quantities we are working with, two length scales appear clearly: one set by the current (the diffusion length I^{-1}), the other by ϵ. This amounts to say that

the effective surface tension decreases with the bulk concentration of metal cations.

To summarize, we have reported here for the first time a 2D realistic mean-field model which reproduces fairly well the structural characteristics of DBM patterns in thin cell ECD. This approach is supported by experimental observations and also reproduces the strong porosity of the deposit obtained in diffusion-limited growth regimes. Despite such, the mean-field model does not capture the microscopic texture of the deposits. It predicts the order of magnitude of the porosity, the average distance between branches, and their high sensitivity to fluctuations.

[1] P. Meakin, *Fractals, Scaling and Growth far from Equilibrium,* Cambridge Nonlinear Science Series, Vol. 5 (Cambridge University Press, Cambridge, England, 1998).
[2] C. Léger, J. Elezgaray, and F. Argoul, Phys. Rev. E **58**, 7700 (1998).
[3] C. Léger, J. Elezgaray, and F. Argoul, Phys. Rev. Lett. **78**, 5010 (1997).
[4] D. A. Kessler, J. Koplik, and H. Levine, Adv. Phys. **37**, 255 (1988).
[5] O. Zik and E. Moses, Phys. Rev. E **60**, 518 (1999).
[6] V. Fleury, M. Rosso, J.-N. Chazalviel, and B. Sapoval, Phys. Rev. A **44**, 6693 (1991).
[7] M. Bazant, Phys. Rev. E **52**, 1903 (1995).
[8] W. W. Mullins and R. F. Sekerka, J. Appl. Phys. **34**, 323 (1963).
[9] J. A. Warren and J. S. Langer, Phys. Rev. A **42**, 3518 (1990).
[10] D. G. Grier, D. A. Kessler, and L. M. Sander, Phys. Rev. Lett. **59**, 2315 (1987).
[11] D. G. Grier and D. Mueth, Phys. Rev. E **48**, 3841 (1993).
[12] J. K. Lin and D. G. Grier, Phys. Rev. E **54**, 2690 (1996).
[13] C. Léger, J. Elezgaray, and F. Argoul, Phys. Rev. E (to be published).
[14] Y. Saito and T. Ueta, Phys. Rev. A **40**, 3408 (1989).
[15] F. Liu and N. Goldenfeld, Phys. Rev. A **42**, 895 (1990).
[16] O. Shochet and E. Ben-Jacob, Phys. Rev. E **48**, R4168 (1993).
[17] Y. Tu and H. Levine, Phys. Rev. E **52**, 5134 (1995).
[18] T. A. Witten and L. M. Sander, Phys. Rev. B **27**, 5686 (1983).
[19] J. Huth, H. Swinney, W. McCormick, A. Kuhn, and F. Argoul, Phys. Rev. E **51**, 3444 (1995).
[20] J.-N. Chazalviel, M. Rosso, E. Chassaing, and V. Fleury, J. Electroanal. Chem. **407**, 61 (1996).
[21] J. Elezgaray, C. Léger, and F. Argoul, J. Electrochem. Soc. **145**, 2016 (1998).
[22] H. Weidong, G. Xingguo, and Z. Yahoe, J. Cryst. Growth **134**, 105 (1993).
[23] J. Newman, *Electrochemical Systems* (Prentice-Hall, Englewood Cliffs, NJ, 1991).